A new opportunity for biomagnetic monitoring of particulate pollution in an urban environment using tree branches

Accepted Manuscript

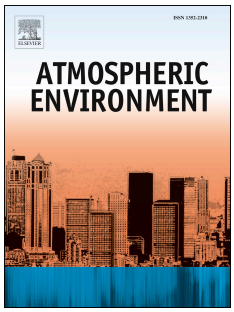

A new opportunity for biomagnetic monitoring of particulate pollution in an urban environment using tree branches

Karen Wuyts, Jelle Hofman, Shari van Wittenberghe, Gert Nuyts, Karolien DE. Wael, Roeland Samson

PII: S1352-2310(18)30461-8

DOI: 10.1016/j.atmosenv.2018.07.014

Reference: AEA 16120

To appear in: *Atmospheric Environment*

Received Date: 25 January 2018

Revised Date: 12 June 2018

Accepted Date: 9 July 2018

Please cite this article as: Wuyts, K., Hofman, J., van Wittenberghe, S., Nuyts, G., Wael, K.D., Samson, R., A new opportunity for biomagnetic monitoring of particulate pollution in an urban environment using tree branches, *Atmospheric Environment* (2018), doi: 10.1016/j.atmosenv.2018.07.014.

A NEW OPPORTUNITY FOR BIOMAGNETIC MONITORING OF PARTICULATE POLLUTION IN AN URBAN ENVIRONMENT USING TREE BRANCHES

Karen WUYTS[1*], Jelle HOFMAN[1], Shari VAN WITTENBERGHE[1,2], Gert NUYTS[3], Karolien DE WAEL[3], Roeland SAMSON[1]

[1]Lab of Environmental and Urban Ecology, Research group Environmental Ecology & Microbiology (ENdEMIC), Dept. Bioscience Engineering, University of Antwerp. Groenenborgerlaan 171, 2020 Antwerp, Belgium. karen.wuyts@uantwerpen.be, jelle.hofman@uantwerpen.be, roeland.samson@uantwerpen.be

[2]Current address: Laboratory of Earth Observation, Valencia University. Catedrático José Beltran 2, 46980 Paterna (Valencia), Spain. shari.wittenberghe@uv.es

[3]AXES Research Group, Dept. Chemistry, University of Antwerp, Groenenborgerlaan 171, 2020 Antwerp, Belgium. gert.nuyts@uantwerpen.be, karolien.dewael@uantwerpen.be

[*]Corresponding author: Lab of Environmental and Urban Ecology, Research group ENdEMIC, Dept. Bioscience Engineering, University of Antwerp. Groenenborgerlaan 171, 2020 Antwerp, Belgium. Tel: +32 3265 3452, Fax: +32 3265 3225. karen.wuyts@uantwerpen.be

Abstract

Environmental magnetism, and the magnetic leaf signal in particular, is amply investigated and applied as proxy for atmospheric particulate matter pollution. In this study, we investigated the magnetic signal of annual segments of tree branches, and the composition of particles deposited hereon. Branches are, contrary to leaves, available during leaf-off seasons and exposed to air pollution year-round. We examined the intra- and inter-tree variation in saturation isothermal remanent magnetization (SIRM) of branch internodes of London plane (*Platanus x acerifolia* Willd.) trees in an urban environment. The branch SIRM, normalized by surface area, ranged from 18 to 650 x 10^{-6} A; the median amounted to 106 x 10^{-6} A. Most of the branch magnetic signal was attributed to the epidermis or bark, and the presence of metal-containing particles on the branch surfaces was confirmed by SEM-EDX. The location of the trees and the height, depth in the crown and the age of the branches significantly influenced the branch SIRM. The median branch SIRM was up to 135% higher near a busy ring road than in quiet environments (city park and quiet street canyon), and was linked to the presence of Fe-rich particles with co-occurrence of trace metals such as Cr, Cu, Zn and Mn on the branch surface. Within the tree crowns, the branch SIRM generally decreased with increasing height, and was 22% higher in the interior than at the periphery of the crowns. Within the branches, the SIRM increased with each year of exposure, but did not relate to year-to-year variation in particle concentrations due to branch surface changes (epidermis shedding). Our results provide indications that branches can be a valuable alternative for biomagnetic monitoring of particulate pollution, but intra-tree variability in branch SIRM can be substantial due to the branch's location in the tree and branch age.

Keywords environmental magnetism, urban trees, air quality, particulate pollution, branch bark

Highlights

- We measured magnetization (SIRM) of urban-tree branches as proxy for particulate deposition.
- Branch SIRM, mainly confined to the bark surface, increases with each year of exposure.
- Branch SIRM reveals similar spatial intra- and inter-tree variation patterns as leaf SIRM.
- Branches can be a valuable alternative for biomagnetic monitoring with leaves.

Funding sources

The study was carried out using the facilities and instruments of the University of Antwerp. This research did not receive any specific grant from funding agencies in the public, commercial, or not-for-profit sectors.

Declarations of interest: none.

1. Introduction

Since the pioneering work by Schädlich et al. (1995) and Matzka & Maher (1999), ample studies have investigated the utility of magnetic biomonitoring with plant leaves for particulate matter (PM) concentration assessment and high resolution spatial mapping. Indeed, leaf magnetic properties such as magnetic susceptibility and saturation isothermal remanent magnetization (SIRM) have shown to vary between land-use classes (e.g., green area vs. urban area and industry; Kardel et al. 2012; Castanheiro et al. 2016), with distance to sources such as traffic-bearing roads, railways and industry (Moreno et al. 2003; McIntosh et al. 2007; Szönyi et al. 2008; Hansard et al. 2011; Kardel et al. 2012) and with motorized-traffic intensity or volume (Moreno et al. 2003; Mitchell & Maher 2009; Kardel et al. 2012). Although direct relationships between atmospheric PM concentrations and leaf magnetic measures are difficult to disentangle for short time periods (Hofman et al. 2014d, but see Mitchell et al. 2010), it has been shown that leaf SIRM correlates significantly with cumulative daily average atmospheric PM_{10} and $PM_{2.5}$ concentrations (Kardel et al. 2011, Hofman et al. 2014d) and the total mass of particles accumulated on the leaf surface (Muxworthy et al. 2003, Hofman et al. 2014c). As such, leaf SIRM is considered a good proxy for time-integrated PM exposure. Leaves of deciduous trees thus provide us with an indication of PM exposure throughout the in-leaf season only, typically from April or May up to October in temperate climates. Leaves or needles of evergreen species could give an indication of PM exposure over longer time periods (Lehndorff et al. 2006) but then the needle exposure time is difficult to ascertain. Moreover, in temperate climate zones, evergreen species are not common in urban environments. Plant parts, other than leaves, exposed to air pollution year-round, are branch and trunk bark. The use of bark in magnetic biomonitoring seems feasible as analyses of particles collected by wiping tree bark with moist tissues demonstrate 50 and 200 times higher magnetization for branch and trunk bark than for leaves (Flanders 1994). However, research on bark magnetic properties is far less abundant than for leaves and is restricted to trunk bark. Kletetschka et al. (2003) and Zhang et al. (2008) used magnetic properties of tree trunk bark as indicators for particles from a traffic-intensive road or an iron-smelting factory, respectively. While trunk bark exposure time to air pollution would be either total tree age or difficult to determine in trunk bark shedding species (e.g., the common urban tree London plane (*Platanus* sp.)), branch bark exposure time is easy to assess.

Here we present the results of a study on the magnetic analysis of branches of a deciduous tree species in an urban context. The aim of the study was (i) to evaluate the potential of the magnetic signal of tree branches for monitoring of particle accumulation and (ii) to identify the variables to take into consideration when using the magnetic signal of branches in future studies, by investigating its spatial intra- and inter-tree variation and its response to increasing branch age. We

measured the SIRM of branch internodes of London plane (*Platanus* x *acerifolia* Willd.) trees in a city center and scanning electron microscopy with energy dispersive X-ray spectroscopy (SEM-EDX) was used to investigate the branch surfaces and the particles present hereon. We hypothesize that magnetic particles are deposited on the epidermis of shoots (or bark in case of older branches), similar to leaves, and that, as such, branch SIRM reveals similar spatial intra- and inter-tree variation patterns as exhibited by leaf SIRM. Lastly, we assume that the deposited magnetic particles accumulate on branches throughout years of exposure.

2. Material & methods

2.1. Sampling set-up

We used London plane (*Platanus* x *acerifolia* Willd.), a deciduous tall tree species, because (i) it is the most common roadside and park tree in many cities in the temperate regions, (ii) branches developed in subsequent years can easily be distinguished and (iii) the *Platanus* sp. have been used before in many biomagnetic monitoring studies using leaves (e.g. Moreno et al. 2003; McIntosh et al. 2007; Hofman et al. 2013, 2014a, 2014c, 2014d). Sampling was performed in the central and southern part of Antwerp city center, Belgium (Fig. 1), in 2012. The city of Antwerp houses 516 000 inhabitants (2015) on 205 km². It encompasses residential and commercial areas in the centre and a busy port and harbor area with petrochemical industries in the north. The city centre is surrounded by a heavily trafficked ring motorway of six to ten lanes, connected with international motorways. The city daily suffers serious traffic congestions. The city experiences a maritime temperate climate. In the city centre, an urban background and roadside air quality monitoring station returned yearly mean atmospheric $PM_{2.5}$ and PM_{10} concentrations of, respectively, 17 and 27 µg m^{-3}, and 19 and 30 µg m^{-3} (Flanders Environment Agency 2013).

We sampled four London plane trees at three locations. The first two trees were located in the quiet street canyon *De Villegas* in a densely populated area: one tree in row of trees halfway the street canyon (Tree 1; 51°11'45.9"N, 4°25'26.1"E) and a second solitary tree on a roundabout at the end of the street (Tree 2; 51°11'47.8"N, 4°25'24.9"E). The traffic intensity in the street canyon itself is very low and is limited to passenger cars (daytime average of 50 vehicles h^{-1}; Hofman et al. 2014a, SGS 2010). Further, we selected a solitary tree in the urban park *Stadspark* (Tree 3; 51°11'31.1"N 4°25'17.0"E), at 150 to 200 m from roads with low (200 vehicles h^{-1}) and medium traffic intensity (730 to 1300 vehicles h^{-1}) and at 250 m from tram lines. Lastly, a solitary tree (Tree 4; 51°12'44.4"N, 4°24'51.8"E) was chosen at an intersection of three traffic-intensive roads. The tree is located at 2 m from the seven-lanes regional ring road *Binnensingel* (daytime average of 1909 vehicles h^{-1}; SGS 2010), at 40 m from the national N1 road from Antwerp to Brussels (daytime

117 average of 2133 vehicles h^{-1}; SGS 2010) and at 70 m from the twelve-lanes highway ring road R1
118 (daytime average of 8400 vehicles h^{-1}; SGS 2010). The train railway line 59 from Antwerp to Ghent
119 is at 25 m from Tree 4. Air quality maps modelled following a IFDM-OSP model chain (Vranckx &
120 Lefebvre 2013) suggest yearly mean $PM_{2.5}$ concentrations of 18, 18 and 21 µg m^{-3}, PM_{10}
121 concentrations of 28, 28 and 31 µg m^{-3} and NO_2 concentrations of 46, 39 and 89 µg m^{-3} in the quiet
122 street canyon, the park and the ring road locations, respectively.

123

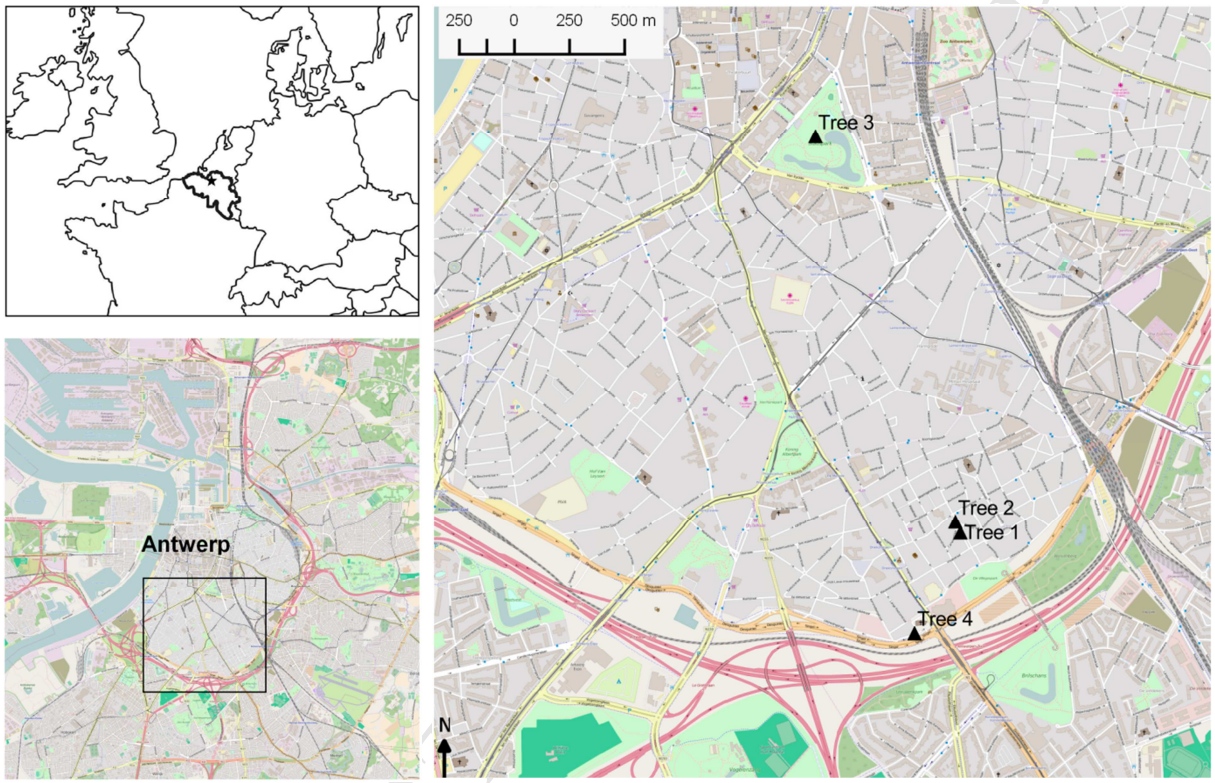

124 *Figure 1. Location of the city of Antwerp (indicated by the star) in Belgium, Europe, and location of the four*
125 *London plane trees sampled in the city of Antwerp (Source: OpenStreetMap contributors,*
126 *https://www.openstreetmap.org/)*

127

128 Tree branches were sampled with a boom lift at 20 sampling positions in the crown of each tree
129 between 11 and 14 September 2012, after a rain-free period of 11 days. From each tree, branch
130 samples were taken at three sampling heights (at about 3.5, 8.5 and 13.5 m above the ground) and in
131 four wind sectors of the canopy (azimuth). All branches were cut at the periphery of the crown, but
132 at 3.5 and 8.5 m height, branches were sampled also inside the crown, i.e., at halfway the tree trunk
133 and the crown periphery. At each sampling position (20 per tree, and thus 80 in total), two branches
134 about 100 cm in length and carrying fresh leaves were collected. Although London plane sheds
135 thick scales of bark on the trunk and the very thick, primary branches, the smaller branches do not

show signs of significant bark loss and have relatively smooth bark tissue in comparison with trunk bark when inspected with the naked eye. The branches were labelled and transported in plastic boxes to the lab for further analyses.

2.2. Sample preparation and magnetic analysis

Arrived in the lab, the branches were stored in cardboard boxes in a cooling room, awaiting further sample handling in random order in 2013. In the lab, the internodes were cut from the branches using secateurs, hereby excluding the leaves, fruits, buds, nodes, and leaf scars. Prior tests, by comparing branch magnetism of trial material before and after it was cut in multiple tiny pieces, revealed no significant contamination by the secateurs.

First, two pretests were performed before all other branches were processed. A first pretest was performed to test for the variation within branches, i.e. between years of development (i.e., consecutive internodes) and between positions of the internode within a year of development (top, mid and base). Therefore, a detailed sampling on a subset of the branches (the bottom branches of Tree 4 at the ring road) was done, by cutting the top, mid and base internodes separately from branches developed in six subsequent growing seasons, i.e., from the current-year branches (Y_0) up to branches developed seven years ago (Y_7). A second pretest was performed to evaluate the contribution of the inside tissue (wood) and the outside surface area (bark) to the magnetic signal. For this, 12 branch internodes were selected from all azimuths, both crown depths and from Y_0, Y_1 and Y_2 years of development of Tree 4, the bark was removed, and bark and wood were magnetically analysed separately.

Second, from all other branches, we cut the internodes developed during the current growing season (Y_0) from each branch, and if possible, the internodes developed during the preceding two growing seasons (Y_1 and Y_2). For each year of development (or branch age), one sample was prepared which consisted of either (i) all internodes developed in that year (in case four or less internodes were available) or a subset of the top, a mid and the base internodes (in case five or more internodes were available).

The internode surface areas were calculated from the length $l_i$and the mean of two diameters (from both ends) $\bar{d}_i$ of the internode determined with a digital caliper (sensitivity 0.01 mm), assuming a cylindrical shape. The exposed branch surface area of a sample is the sum of the surface areas of each internode i involved in the sample (with k the total number of internodes in the sample):

$$\sum_{i=0}^{k} l_i * \bar{d}_i * \pi$$

Prior to magnetic analyses, the internodes of each sample were cut into pieces, tightly packed in cling film and pressed in a plastic container (10 cm^3). Magnetic susceptibility measurements, conducted with the MS2 with B sensor from Bartington Instruments, were below the detection limit of the instrument (2 x 10^{-6} SI). Following the protocol described by Kardel et al. (2011), the container holding the sample was magnetized in a pulse DC magnetic field of 1 Tesla using a Molspin pulse magnetizer (Molspin Ltd, UK) and the saturation isothermal remanent magnetization (SIRM) was measured twice immediately after magnetization using a Molspin Minispin magnetometer (with sensitivity 10^{-9} A m^2). The magnetometer was calibrated with a magnetically-stable rock, and its accuracy was checked every ten samples using the same rock specimen as reference sample. Method blanks were included as empty containers. The measured magnetization values (in mA m^{-1}) were multiplied by 10^{-5} m^3 (the assumed sample volume of the Minispin) to obtain the magnetic moment (A m^2), which was then normalized by dividing by the exposed branch surface area of the sample, yielding an area-normalized SIRM value expressed as A. The magnetic analyses of the pretests were performed in 2013; the other magnetic analyses were done in 2014.

The SIRM value of a branch is considered an assemblage of SIRM values accumulated throughout the different years of exposure, starting from the year of development, and thus SIRM values owing to a specific year can be estimated by comparison of subsequently-developed branches. However, the magnetic particles deposited on branches during previous year(s) are 'diluted' in the SIRM of the following year(s) because the branch bark expands as a result of branch diameter growth. So, to evaluate the year-to-year variation, we estimated the annual increase in SIRM taking into account the yearly branch area expansion induced by diameter growth. Therefore, we estimated the mean SIRM owing to the year of development of a branch ($SIRM_{t=y}$; with y from 2007 to 2011) as the difference between the median normalized SIRM value of the given branch with age k ($SIRM_k$) and the normalized SIRM value of the branch developed the next year (i.e. with one year lower branch age; $SIRM_{k-1}$) multiplied by the ratio of median diameter of the given branch (d_k) to the median diameter of the branch developed the next year (d_{k-1}), i.e. corrected for bark expansion due to diameter growth during one year:

$$SIRM_{t=y} = SIRM_k - SIRM_{k-1} * \frac{d_k}{d_{k-1}}$$

with y between 2007 and 2011 and k (= 2012-j) the branch age (between 1 and 5).

2.3. SEM-EDX analyses

On a subset of stored samples, SEM-EDX was performed. For each branch age (Y_0, Y_1 and Y_2), two replicates were chosen from the branch positioned at the bottom, south and inner side of the crown of Tree 2 in the quiet street canyon, Tree 3 in the city park and Tree 4 at the busy ring road. In addition, Y_5 branches were selected from Tree 3, taken from the same sampling position. The epidermis and bark of the shoots were cut in 2 mm wide strips from all-round the dried samples, were fixed on metallic pin stubs with double-sided tape and vacuum-coated with carbon (10 nm; Leica EM ACE600) to reduce charge build-up effects. The samples were examined with a Field Emission Gun – Environmental Scanning Electron Microscope (FEG-ESEM) equipped with an Energy Dispersive X-Ray (EDX) detector (FEI Quanta 250, USA; at AXES and EMAT research groups, University of Antwerp), using an accelerating voltage of 15kV, a take-off angle of 30°, a working distance of 10 mm and a chamber pressure of 10^{-4} Pa. Imaging was performed based upon secondary electrons (SE), back-scattered electrons (BSE) and characteristic X-rays (EDX). For the latter, elemental distribution maps (30 frames) were recorded with a 4.5 µm spot size, at a magnification of 5000, a resolution of 512 x 352, and with a dwell time of 10 µs per pixel, resulting in a total scan duration between 800 – 2000 s. Based on the BSE image, three to four particles were selected of which an EDX point spectrum was acquired, using a dwell time of 50 s per spectrum. All EDX data analysis was performed by using the Inca software package (Oxford Instruments).

2.4. Statistical analysis

To test for the variation within branches, i.e. between years of development and between internode positions (top, mid and base), we fitted a hierarchical linear mixed-effects model on the detailed subset data of the lowest sampling height of tree 4. Values of internodes developed six and seven years ago were removed, due to the low amount of replicates, and 125 data points were retained. The model included the year since development (further on called ‘branch age’; six years, from zero to five), the internode position (base, mid, top) and their interaction as fixed factors, while sampling position and branch, nested in the latter, were included as random factors. Pearson correlation analyses were performed between the median SIRM values of branches developed in the year 2007 up to 2012 and the time of exposure (in number of months, assuming bud break and shoot development occurs each year in the second part of April). Also correlations were analysed between the median SIRM values of branches developed in the year 2007 up to 2012 and the mean SIRM owing to the year of development of a branch in the year 2007 up to 2012 on the one hand and the yearly mean $PM_{2.5}$ and PM_{10} concentrations measured in the nearest air quality monitoring station for urban background, at 2.0 km from Tree 4, for the corresponding years on the other hand (station Borgerhout R801; Flanders Environment Agency 2017).

To test for the variation between trees, within trees and within branches, the data of all trees (N=374) were fitted with a hierarchical linear mixed-effects model, comprising tree, sampling position nested in tree, and branch nested in sampling position as random factors. Location (three levels: De Villegas street, city park, ring road), sampling height, azimuth (four levels: N, E, S, W), crown depth (two levels: crown interior or periphery), year since development (or branch age) and their two-way interactions were included as fixed factors.

All statistical analyses were performed in R 3.2.2 (R Core Team 2015). The linear mixed models were built on ln-transformed SIRM data using the package nlme (Pinheiro et al. 2015). When building the models, first the structure of the random factors was optimized, and then the contributions of the fixed factors and their interactions to the model were investigated. The Akaike Information Criterion was used to compare performances of different model structures. The residuals of the linear mixed models were checked for normality and plotted against explanatory variables to check for bias, and the models were evaluated using diagnostic plots. Graphs were produced using R package ggplot2 (Wickham 2009) and contour plots were developed using linear interpolation with R package akima (Akima & Gebhardt 2015).

3. Results

3.1. Magnetic analyses

3.1.1. Detailed within-branch variation pretests

The first pretest (detailed analysis of the data subset of Tree 4) showed that the year since development significantly ($p<0.05$) affected the ln-transformed branch SIRM value (Table 1), with the branch SIRM increasing with branch age. The branch SIRM varied from 161 (± 49) x 10^{-6} A for Y_0 branches to 473 (± 373) x 10^{-6} A for Y_5 branches (median ± median absolute deviation or MAD; Fig. 2). The estimations of SIRM owing to the year of development of a branch amounted to 161, 147, 49, 184, 32 and 115 x 10^{-6} A for Y_0 (in 2012), Y_1, Y_2, Y_3, Y_4 and Y_5 (in 2007) branches respectively. Thus, with each year of development, the branch SIRM on average increased by 115 x 10^{-6} A. With median values of 232 (± 123), 266 (± 146) and 280 (± 134) x 10^{-6} A at the base, mid and top of the branches, the internode position within a year of development did not significantly influence the SIRM of that internode (Table 1, Fig. 2). The interaction between the year since development and the internode position did not significantly ($p>0.05$) contribute to the model and was removed. The median branch SIRM values from branches developed in 2007 up to 2012 correlated significantly and positively with (i) the time of exposure in months ($r=0.97$, $p=0.0018$) and (ii) the yearly mean $PM_{2.5}$ ($r=0.90$, $p=0.0134$) and PM_{10} ($r=0.89$, $p=0.0171$) concentrations

measured at the nearest air quality monitoring station in the corresponding years. Relationships of the mean SIRM owing to the year of development of a branch in the year 2007 up to 2012 and the yearly mean $PM_{2.5}$ and PM_{10} concentrations were not significant (r=-0.42, p=0.4100 and r=-0.35, p=0.4990).

The second pretest in which bark and wood were analysed separately revealed that, on average (N=12), 86% of the total bark + wood SIRM signal is attributed to the bark, while the latter only represents 34% of the wood + bark mass in a shoot sample. For Y_0, Y_1 and Y_2 internodes, bark represented 78, 88 and 93% of the total bark + wood SIRM signal.

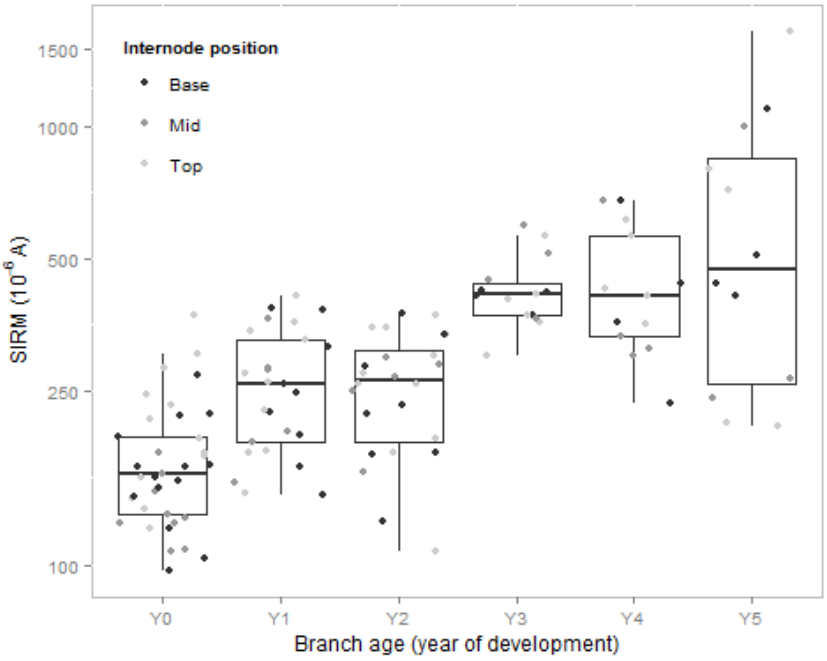

Figure 2. SIRM (10^{-6} A) values of branch internodes, including the median, according to the year of development of the branch, from current-year branches (Y0) up to five-year old branches (Y5)

Table 1. ANOVA of the fixed factors in the linear mixed models fitted to (a) the detailed subset data of tree 4 to look into intra-branch variation and (b) the full dataset comprising all trees to look into inter-tree, intra-tree and intra-branch variation.

Dataset	Source of variation	F value	p value
Detailed sub-dataset on Tree 4 (N=125)	(Intercept)	14546	<0.0001
	Internode position	2.53	0.0845
	Branch age	101.9	<0.0001
Full dataset (N=374)	(Intercept)	19473	<0.0001
	Location	50.7	<0.0001

Height	16.2	0.0002
Azimuth	0.26	0.8572
Crown depth	13.4	0.0005
Branch age	101.6	<0.0001
Location x Height	6.2	0.0036
Location x Azimuth	1.2	0.3393

281

282

283 3.1.2. Variation between trees, within trees and within branches

284 From all four trees in total, we were able to collect and magnetically analyse 149 samples of
285 current-year branches, 126 samples of one-year old branches and 99 samples of two-year old
286 branches. The median (± MAD) SIRM value of all branches taking into account all branch ages,
287 locations, heights, azimuths and crown depths amounted to 106 (± 72) x 10^{-6} A, with minimum and
288 maximum values of 18 and 650 x 10^{-6} A.

289 When considering the current-year branches at the crown periphery (Fig. 3), large variation can be
290 observed between trees and within trees according to height and azimuth. The median branch SIRM
291 of current-year periphery branches was 58 and 46 x 10^{-6} A for the solitary tree (Tree 1) and row tree
292 (Tree 2) in the street canyon, 56 x 10^{-6} A for the park tree (Tree 3) and 108 x 10^{-6} A for the ring
293 road tree (Tree 4). While the within-tree variation in branch SIRM was low in both street-canyon
294 trees (Tree 1 & 2; MAD= 22 and 26 x 10^{-6} A) and the park tree (Tree 3; MAD=16 x 10^{-6} A), distinct
295 variation was observed in the ring road tree (Tree 4; MAD=54 x 10^{-6} A), particularly in relation
296 with height. Although the one- and two-year old branches in the crown periphery showed higher
297 SIRM values, analogous patterns as in current-year branches can be observed.

298

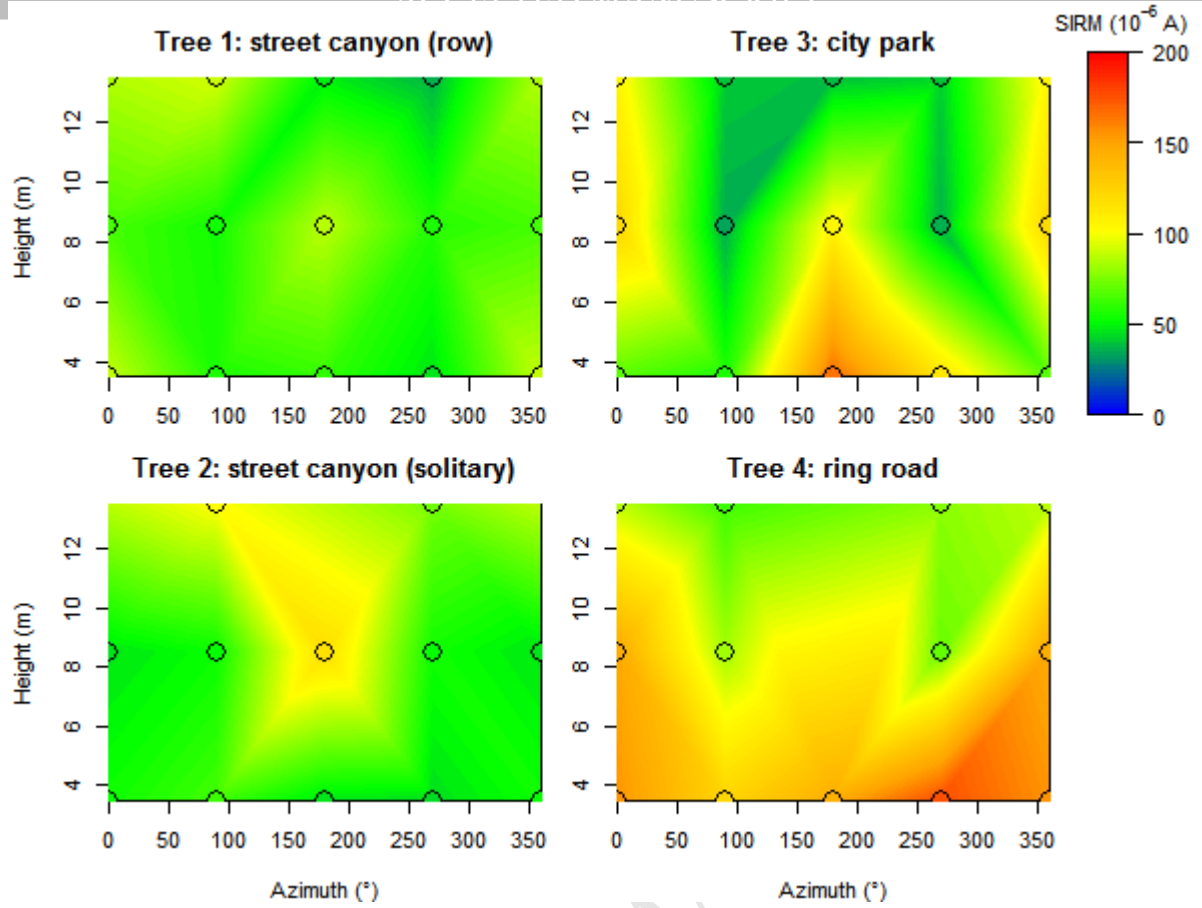

Figure 3. SIRM (10^{-6} A) of the current-year branches (Y0) at the crown periphery of the four trees sampled in the quiet street canyon De Villegas (Tree 1 & 2), in the city park (Tree 3) and at the Ring road (Tree 4). The data on the sampling positions (indicated by circles) are means of two branches, collected at the N (0°=360°), E (90°), S (180°) and W (270°) sides of the trees and at 3.5, 8.5 and 13.5 m height, and are linearly interpolated using the akima package in R.

When building the linear mixed-effects model for the full dataset including all trees, the random factors tree and branch did not significantly increase model performance. The sampling position in the crown explained 15% of the total data variance. From all two-way interactions of the fixed factors, only the location x height interaction was retained in the final model. The location of the trees, the height and depth in the canopy and the year of branch development significantly influenced the branch SIRM (Table 1). The effect of tree location, height in the crown and the year of branch development are depicted in Figure 4. Differences were observed between the three locations, in the following order: the quiet street canyon < city park < the Ring road (Fig. 4), but only street canyon and city park values differed significantly from the ring road tree values. In general, the median branch SIRM was 18% higher at the city park and 135% higher at the ring road in comparison with the quiet street canyon. Within the tree crown, the branch SIRM showed in general a significant, decreasing trend with increasing height. The median branch SIRM at 8.5 and

13.5 m height was 24 and 27% lower than at 3.5 m. The height effect depended significantly on location (Fig. 4). Significantly more pronounced height effects were appreciable at the Ring road (61% lower at 13.5 m than at 3.5 m) and in the city park (37% lower at 13.5 m than at 3.5 m) than in the street canyon, where the height effect even was negligible (3% higher at 13.5 m than at 3.5 m). In addition, the crown depth (crown interior versus crown periphery) significantly affected the branch SIRM within the trees (Table 1), the inside of the crown exhibiting 22% higher SIRM values than the crown periphery (Fig. 5). No significant influence of azimuth in the crown on the branch SIRM was detected (Table 1, Fig. 5). Although azimuth did not interact significantly with location, we did found significantly higher branch SIRM at the E side than at the other sides of the street canyon trees. Within the branches, a significant positive effect of the year since development was observed on the branch SIRM (Fig. 4, Table 1). The median SIRM values of one-year and two-year old branches were 134 and 83% higher, respectively, than those of current-year branches (68 ± 37 x 10^{-6} A).

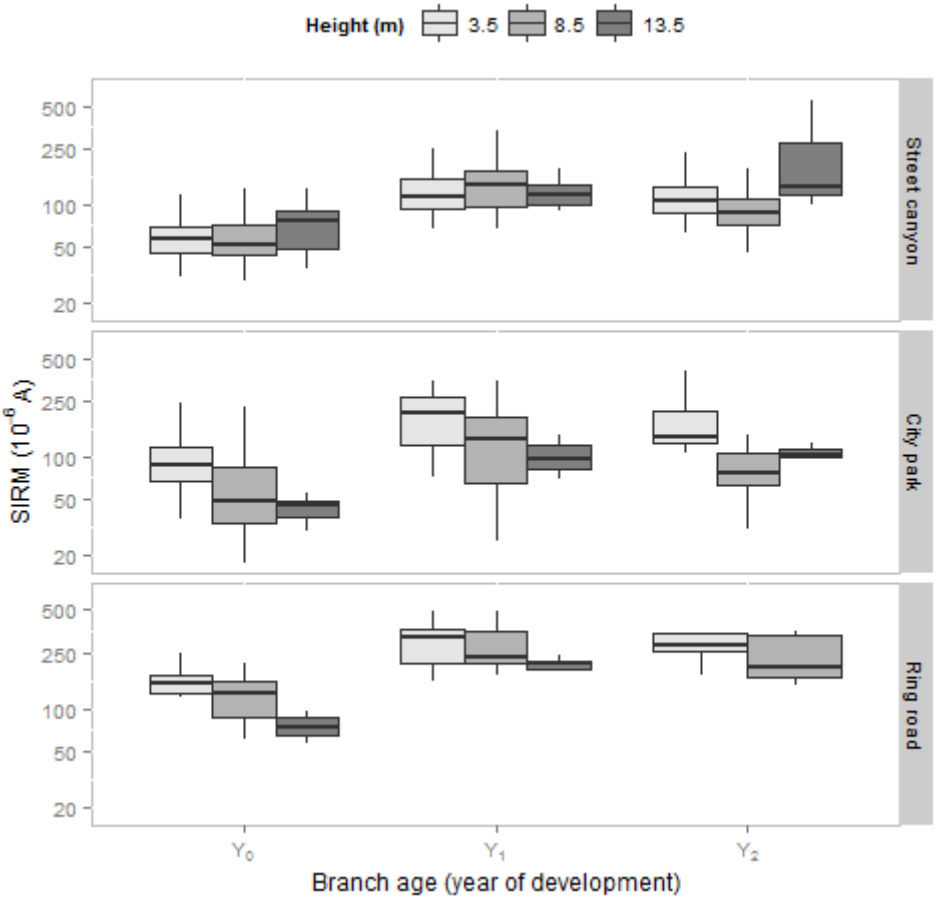

Figure 4. Median SIRM (10^{-6} A), with hinges indicating 25th and 75th percentiles and whiskers 1.5 x the inter-quartile range, at the three studied locations, i.e., the De Villegas street canyon, the city park and the Ring road, measured on current-year branches (Y0), one-year old branches (Y1) and two-year old branches (Y2), sampled at three heights (3.5, 8.5 and 13.5 m). Location ($p<0.0001$), branch age ($p<0.0001$) and

height (p=0.0002) and the location x height interaction (p=0.0036) significantly influenced the branch SIRM (Table 1).

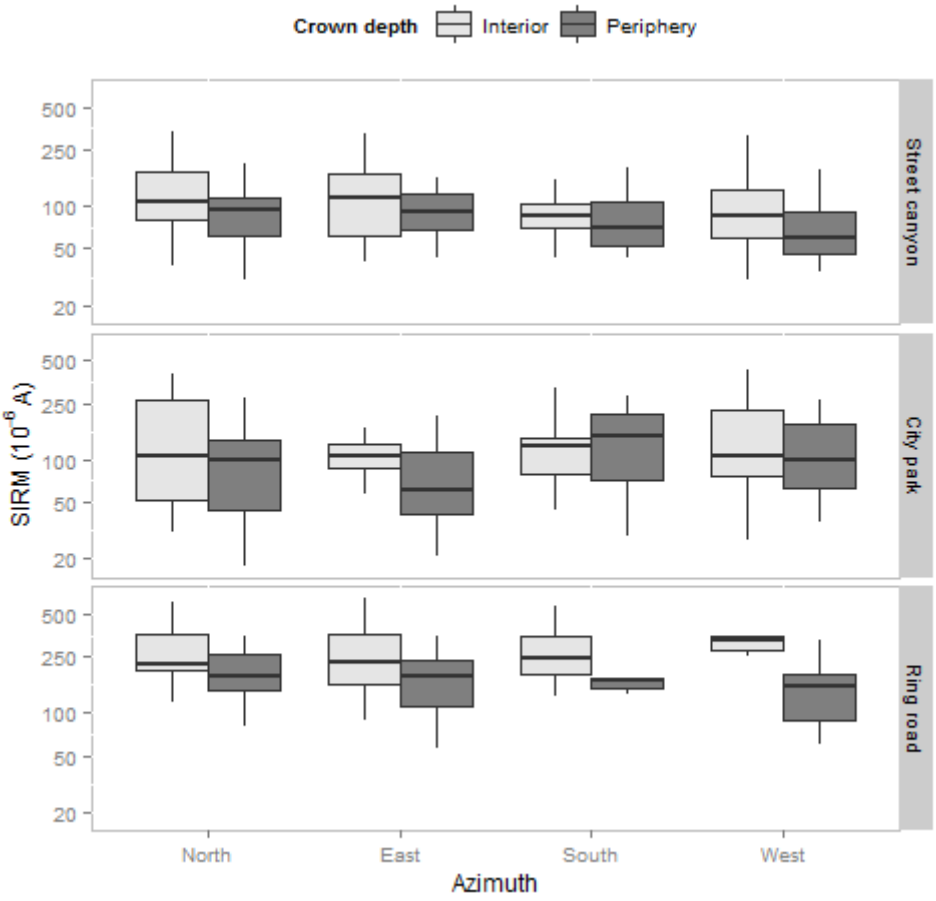

Figure 5. Median branch SIRM (10^{-6} A) (± standard error) as a function of crown depth (crown interior and crown periphery) at the studied crown azimuths (north, east, south and west) for all four trees under study. Location (p<0.0001) and crown depth (p=0.0005) significantly influenced the resulting branch SIRM (Table 1).

3.2. SEM-EDX elemental distribution maps & point spectra

Secondary electrons images show a rather smooth, contiguous epidermis in current-year branches (Fig 6A), while in Y_1 branches the epidermis is cracked and ruptured by fissures and lenticels, revealing the underlying cork cells (Fig 6B and C). In Y_2 branches, the epidermis is ruptured even further (Fig. 6D) and even has come off over large parts of the surface, leaving a rough surface of cork cells (Fig. 6E). In Y_5 branches of Tree 4, the epidermis is shed completely and the branch surface consisting of cork cells is rough and has spongy appearance (Fig. 6F). Back-scattered electrons images (shown in Fig. 7 for Y_1 branches) reveal the presence of particulates of different

shapes and sizes on the epidermis and on and between the spongy cork cells. The branch surfaces of Tree 2 in the quiet street canyon showed more particles than those of Tree 3 in the park and Tree 4 at the ring road. Striking is the abundant presence of particles in the spongy matrix of the cork cells of five-year old branches (Y_5) in Tree 4 (Fig. 7). Visual inspection of the covariation between element maps (shown in Fig. 7 for Y_1 branches) learns that the branch surfaces harbor particles that contain Al and Si with Fe, Mg, K, Na and/or Cl, particles of S with Na and Ca and Fe-rich particles that seem to contain, next to O, almost exclusively Fe. These Fe-rich particles were more abundant on the branch surfaces of Tree 4 at the ring road than the other trees. Chemical composition spectrum analyses of selected particles (Fig. 8) revealed that the Fe-rich particles also contained K, Ca, Mg, Na, Al and Si. In Tree 4 at the ring road, all these Fe-rich particles also contained Cr, Mn, Ti, Zn and Ba and particularly Cu, while in Tree 2 in the street canyon some particles contained Cr, Cu, Mn and Zn. In Tree 3 in the park, this co-occurrence of Fe with trace metals did not occur.

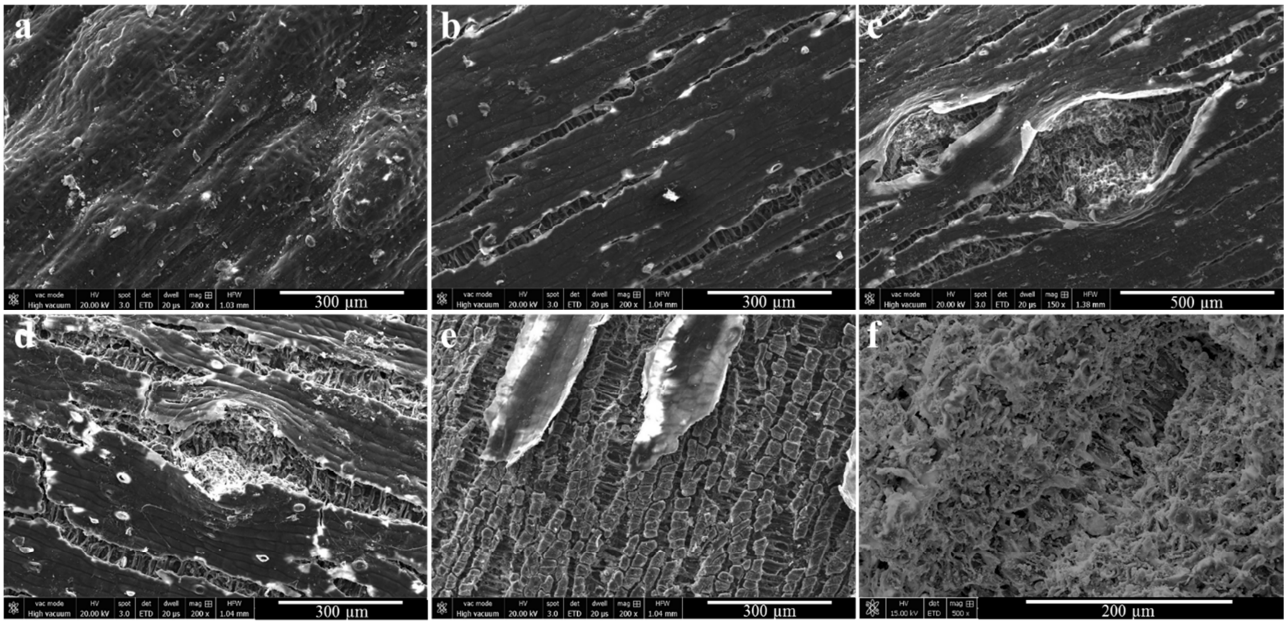

Figure 6. SEM secondary electrons image of the surface of Y0 branches (a), Y1 branches (b and c), Y2 branches (d and e) and Y5 branches (f). All images from park tree (Tree 3) except f from ring road tree (Tree 4).

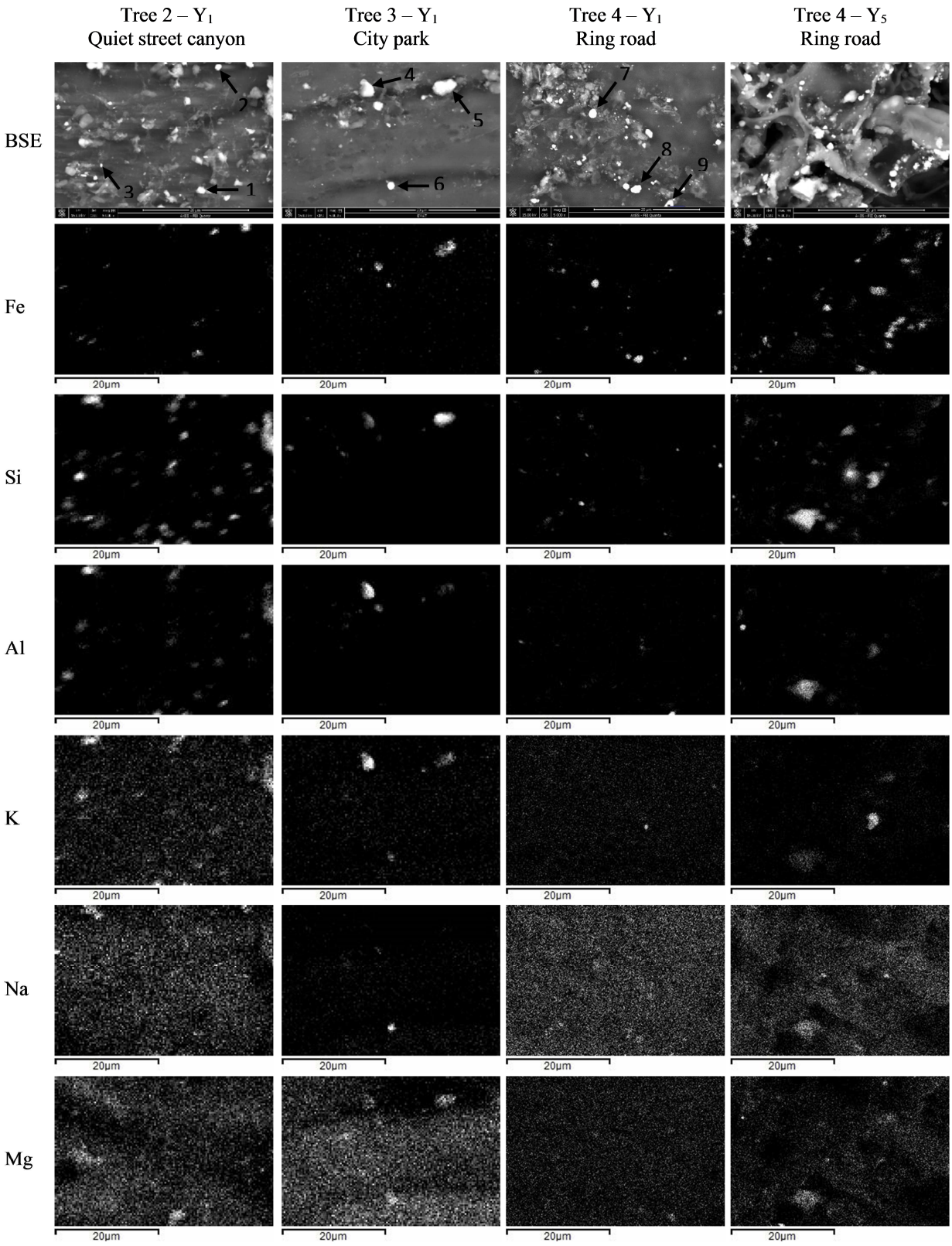

Figure 7. SEM back-scatter electrons images (BSE) and elemental distribution maps of Fe, Si, Al, K, Na and Mg, obtained by EDX mapping, of a Y1 branch of Tree 2 in the quiet street canyon, a Y1 branch of Tree 3 in the city park and a Y1 and Y5 branch of Tree 4 near the ring road (5000x). Arrows indicated the particles analysed by EDX point measurements and numbers refer to the corresponding EDX point spectra in Fig. 8.

375

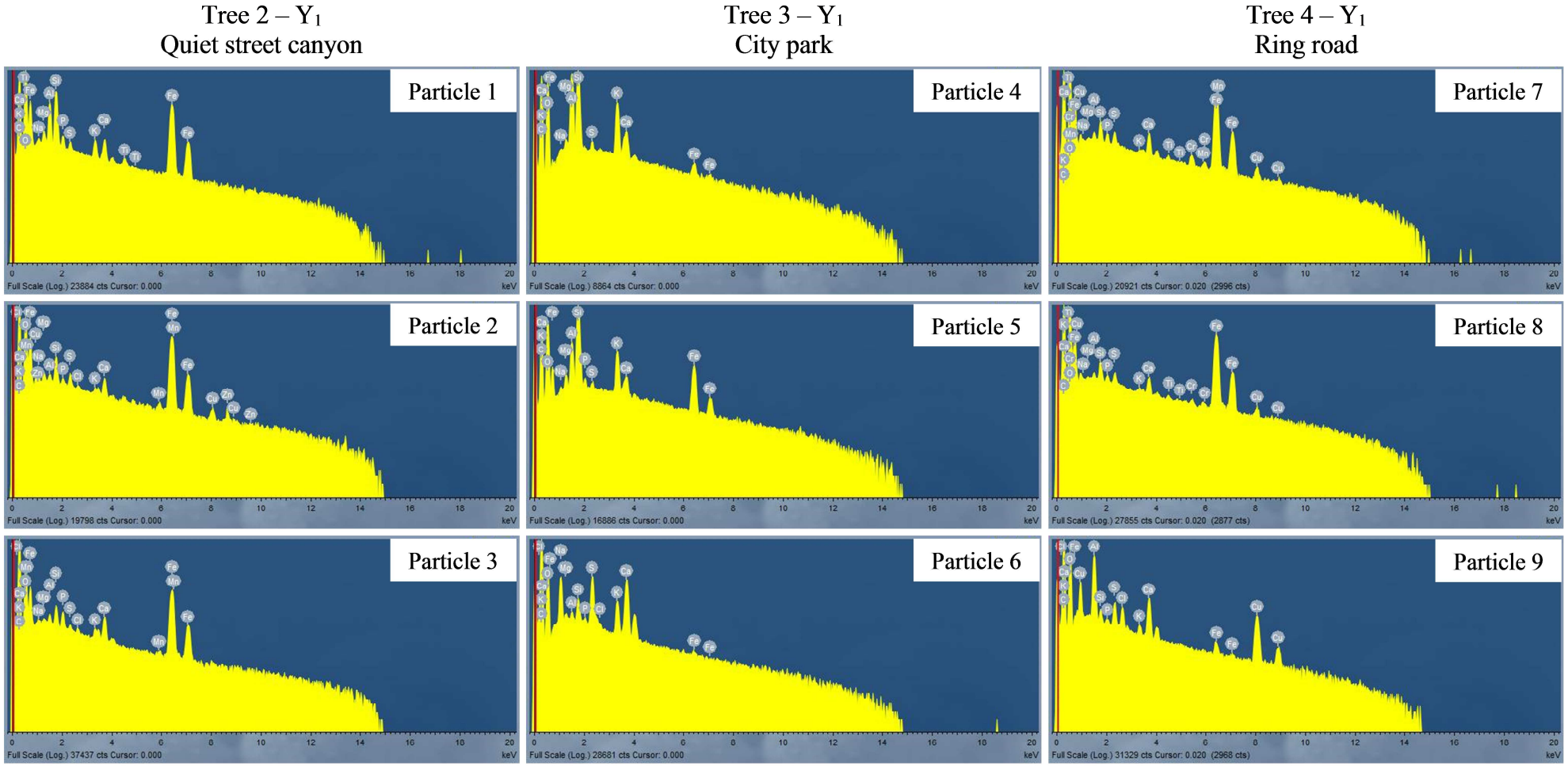

376

377 *Figure 8. EDX point spectra of selected particles on the surface of Y1 branches following SEM-EDX analysis. The numbers refer to the particles indicated in Fig. 7*

4. Discussion

The main portion of the branch SIRM signal obtained in our study seems to be confined to the bark of the branch. This endorses the normalization of the SIRM signal by branch surface area and validates our hypothesis that magnetic particles are deposited on the branch surface, just like on leaf surfaces. This is confirmed by the presence of metal-containing particles on branch surfaces as detected by the SEM-EDX elemental maps and point spectra. We, thus, follow the suggestion made by Zhang et al. (2008) and Kletetschka et al. (2003) that magnetic particles are intercepted and adhered by (branch) bark.

4.1. Between tree variation: location effect

The branch SIRM was able to distinguish between the three locations, particularly between the lower values in the quiet street canyon and the city park on the one hand and much higher values at the ring road on the other hand. For leaves, SIRM has shown to vary between land-use classes (e.g., green area vs. urban area and industry) and with distance to, and intensity of, sources such as traffic-bearing roads, railways and industry and with motorized-traffic intensity or volume (Moreno et al. 2003, McIntosh et al. 2007, Szönyi et al. 2008, Mitchell & Maher 2009, Hansard et al. 2011, Kardel et al. 2012). Furthermore, leaf SIRM has been directly related to exposure to traffic-induced PM, cumulative daily average atmospheric PM_{10} and $PM_{2.5}$ concentrations (Kardel et al. 2011, Hofman et al. 2014d) and the total mass of particles accumulated on the leaf surface (Muxworthy et al. 2003, Hofman et al. 2014c). Also for traffic-related gaseous compounds such as NO_x (McIntosh et al. 2007, Hofman et al. 2014b) and for trace metals incorporated in particles such as Fe, Zn, Pb, Cd and Cu (Sant'Ovaia et al. 2012, Castanheiro et al. 2016) significant relations are found with leaf SIRM, suggesting the influence of the same source i.e. traffic. For branch bark, no such direct relations have been suggested yet, but higher bark SIRM has been observed in tree stems at sides facing towards a smelting factory emitting magnetite-dominated PM (Zhang et al. 2008) and antipodal to a heavy-trafficked highway emitting metallic pollution (Kletetschka et al. 2003). In our study, the higher branch SIRM values at the ring road coincide with higher PM_{10}, $PM_{2.5}$ and NO_x concentrations modelled at high resolution by Vranckx & Lefebvre (2013). Moreover, observed directional (azimuth) and height effects in Figure 3 seem to be associated with, respectively, the location and distance to motorized road traffic.

SIRM is mainly sensitive to ferro(i)magnetic particulates, which can be of natural origin or anthropogenic. Following the guideline of 70% relative humidity suggested by Rodríguez-Germade

et al. (2014), lithogenic dust contributions will be limited and so good correlations can be expected between metals and leaf magnetic signals in our study area (relative humidity between 70 and 90% according to the Royal Meteorological Institute of Belgium, http://www.meteo.be). The SEM-EDX analyses revealed that the branch surface of the park tree and in the quiet street canyon (Tree 2 and 3) mainly collected particles containing a mixture of Si, Al and Fe in combination with K, Mg, Na, S, and Cl (probably Al, Si or Fe oxides or sulfides), which are linked to sea salt, crustal matter and road dust (Viana et al. 2008, Vercauteren et al. 2011). In anthropogenic dust, the Fe in ferri(o)magnetic particles is partly replaced by other cations such as Ni, Co, Cr, Ti, Al, and Mg (Hoffmann et al. 1999). The co-occurrence of Fe with Ni, Cu, Zn, Cr, Cd, and Pb is associated with motorized road traffic (Viana et al. 2008, Vercauteren et al. 2011) due to exhaust emissions and wear and abrasion of brakes, tires and roads (Pant & Harrison 2013). In Tree 4 at the ring road, more Fe-rich particles were observed, which showed traces of Cr, Cu, Mn, Ti, Zn and Ba. In Tree 2 in the quiet street canyon, also Fe-rich particles were present on the branch surface, with some containing trace metals, but they were scarcer. The Fe-rich particles on Tree 3 in the park did not show co-occurrence with traffic-related trace elements. So we can identify as potential source of magnetic particles on Tree 4 the high-intensity motorized traffic on the regional seven-lane ring road right next to the sampled tree (at 2 m), the twelve-lane highway ring road at 80 m and the national N1 road (Antwerp -Brussels) at 50 m. Another source could be the high-intensity train traffic on the railway line Antwerp-Ghent at 25 m, as railroad traffic generates particles high in Fe and Zn content (Castanheiro et al. 2016). The city park tree (Tree 3), with lower branch SIRM values, is located further away from the nearest road (at 150-200 m) and railway line (at 250 m). Trees 1 and 2 in the quiet street canyon showed even lower branch SIRM, and indeed, these trees were located even further from the nearest busy roads and railways (at 250 m from the regional ring road and 450 m from the highway ring road and railway line). The small contribution of the traffic inside the quiet street canyon as source of magnetic particles is indicated by the very small contribution (5%) of the local traffic emissions to the atmospheric PM concentrations in that street canyon (Hofman et al. 2014d). Our study confirms that magnetic properties of branches, just like leaves, allow a quick discrimination between locations that differ in distance from traffic-bearing roads and railways and in modelled atmospheric pollution (PM_{10}, $PM_{2.5}$ and NO_x concentrations) through differences in branch surface-deposited magnetic particulates, but more research is needed to link branch SIRM with exposure to traffic-borne PM. Obviously, a more extensive dataset including more tree repeats per land-use class is necessary in future studies, when aiming at relating the magnetic signal of branches to specific land-use classes.

4.2. Within tree variation: effect of height, azimuth and crown depth

Within the trees, the branch SIRM decreased with increasing sampling height. Similar height effects in the same height range (3.5-13.5 m) are observed for leaf SIRM of plane trees (Hofman et al. 2013, 2014c) and the mass of coarse particles (> 10 µm) collected by leaves in street canyons (Hofman et al. 2014c). In tree ring cores, Zhang et al. (2008) observed height effects on SIRM, but only on the tree side oriented towards the main polluting source, a smelting factory. Hofman et al. (2013, 2014c) attributed the lower leaf SIRM values in the upper canopy to lower atmospheric particulate concentration (as a result of larger distance to the source at street level and increased ventilation) and higher wash-off of leaf-deposited particles (due to increased exposure to rain). Indeed, we observed the most pronounced height effect at the ring road, where the pollution source (high-intensity traffic) is located right next to the sampled tree and where the open character of the area facilitates good ventilation and efficient dilution of the traffic pollution. In the quiet street canyon and in the city park, the source strength of the contributing emission source is weaker due to, respectively, a much lower traffic intensity (street canyon) or higher distance to the road (park), hence explaining the weakened height effect. Unexpectedly, in the street canyon, the SIRM in Y_0 and Y_2 branches suddenly increased at 13.5 m height compared with 8.5 m, which is fully due to Tree 2. The reason for the unexpectedly higher SIRM values at 13.5 m in Tree 2 is unclear, although particle deposits from wind-blown emissions originating from the upwind regional ring road (250 m) and highway ring road (450 m) cannot be excluded.

No significant overall effect of azimuth on branch SIRM was observed. It seems that the azimuthal differences in magnetic-particle deposition vary from tree to tree, probably depending on the local settings of the tree and its surroundings. These settings can be the location (position and distance) of pollution sources relative to the tree (as evidenced by Tree 4 in Figure 3), the tree crown architecture and the wind flow patterns influenced by the architecture of the surroundings, as put forward by Hofman et al. (2014a) as important determinants for azimuthal effects on leaf SIRM. For example, the influence of the local pollution source (intensive traffic) is clearly visible (but not significant) in the bottom branches at the north and west side of the ring road tree, the sides the closest to the seven-lane ring road. Also Matzka & Maher (1999) observed higher SIRM values for leaves at the traffic-oriented side than at the distal side of a *Betula pendula* tree. The higher branch SIRM at the east side of the tree crown in the street canyon complies with the higher leaf SIRM at the north-east side of trees simultaneously sampled in the same street canyon by Hofman et al. (2014c).

Branches sampled on the inside of the tree crowns exhibited higher SIRM values than branches at the crown periphery, thus suggesting higher accumulation of magnetic particles inside the crown.

As wind flow enters a tree crown, from the periphery to the interior, wind speeds are reduced by drag, and turbulence will be increased. With lower wind speeds, deposition velocities and capture efficiencies of branches for fine particles are lowered (Freer-Smith et al. 2004), although gravitational settling and turbulent transfer resulting from impaction and interception processes will be increased for coarser particles (Freer-Smith et al. 2005). The potentially lower deposition rate inside the crown thus must have been counteracted by lower wash-off inside the crown (as these branches are less exposed to rain), additional input of particles via throughfall (canopy drip from branches and leaves above) and/or decreased ventilation and dilution with subsequent build-up of particles in the atmosphere under and inside the tree crown. Although atmospheric-concentration build-up is a plausible explanation for locations where pollution sources are located next to or underneath the trees, such as the ring road location, it cannot hold for the city park and street canyon locations. Our observations thus suggest a significant role of rain in the accumulation of magnetic particles on branches. For leaves at least, the effect of rain on particle accumulation and magnetic signal is ambiguous. While in some studies leaf magnetism and particle accumulation are lowered by rainfall (e.g., Mitchell et al. 2010), in other they are increased (Wang et al. 2015) or not affected at all (e.g., Urbat et al. 2004, Szönyi et al. 2008, Hofman et al. 2014d).

4.3. Within branch variation: effect of branch age

The trend of increasing branch SIRM with branch age (i.e. between subsequently-developed branches) is obvious. This trend could be due to an increasing time of exposure causing the amount of magnetic particles on the branches to accumulate throughout time, to temporal changes in yearly PM concentrations in the corresponding year of branch development and to temporal changes in branch surface structure. The median SIRM values of branches developed in 2007 up to 2012 indeed correlated significantly with the number of exposure months, endorsing the particle accumulation hypothesis. In addition, also significant correlations were observed with the yearly mean $PM_{2.5}$ and PM_{10} concentrations of the corresponding years. However, care should be taken in the interpretation of the latter results: the $PM_{2.5}$ and PM_{10} concentrations gradually and monotonically decreased from 2007 to 2012, and thus the significant correlations between branch SIRM and PM concentrations could just as well be the result of the coincidence of two independent time trends.

By comparing SIRM values of subsequently-developed branches, assuming year-to-year accumulation, and taking into account the dilution effect throughout time due to surface stretching - as was previously shown for leaf SIRM in early leaf development by Hofman et al. (2014d) - we calculated the SIRM owing to the different years of exposure. On average, one year of exposure

caused an accumulation of 115 x 10^{-6} A for branches near the Ring road, although strong variation was experienced. This variation in SIRM owing to specific years cannot be explained by variation in $PM_{2.5}$ and PM_{10} concentrations between the years, since correlations between both were not significant. Thus, when taking into account year-to-year accumulation and the dilution effect throughout time due to surface stretching, no relationship with atmospheric PM concentrations could be observed.

Interestingly, the SEM pictures demonstrated shifts in branch surface structure with time, which could not be observed during sample collection by naked-eye visual inspection. At first, the epidermis of young plane shoots is smooth, but is increasingly ruptured in the next two years. Though thorn, the epidermis accumulates particles from year to year. As the epidermis starts to come off in the second year, the particles on it are disposed of too, while the rougher, initially uncontaminated cork layer is uncovered. The shedding of the epidermis starts in the second year, explaining the smallness of the increase in SIRM from Y_1 to Y_2 branches in Fig. 2 and Fig 4. Throughout the following years, the epidermis shedding progresses and completes, while particles accumulate on the newly revealed cork layer and the SIRM values rise again. Indeed, in the SEM pictures of five-year old branches (Y_5), one can clearly see that particles nest abundantly on and deep in the cork layer. With changing surface roughness (from epidermis to cork layer), rates of deposition and loss of particles from the branches (e.g. by precipitation) are probably altered, but our data is too short to make conclusions on changing particle accumulation rates. The exfoliation of the branch thus discards the hypothesis that the median SIRM of a branch developed in a specific year is representative for the yearly mean PM concentrations in the corresponding year. The increase in SIRM with branch age thus likely is the result of accumulation of particles with increasing time of exposure, interfered by the change in surface structure. The branch SIRM shows a stagnation but not a complete decline to 0 in Y2 or Y3, at a point when the epidermis is almost completely shed, because the exfoliation occurs gradually enabling the cork layer underneath to start accumulating particles before the entire epidermis is completely shed.

Catinon et al. (2009) found young ash trees to accumulate metals in stem bark up to 10 to 15 years, after which the deposited material only slowly increased as if branches were becoming saturated, depending on its exposure to rain wash-off. No signs of saturation were observed in the branch bark of our study (at least up to five-year old branches). In a study on trace elements in the branch bark of holm oak in an urban environment, Drava et al. (2017) observed, in a series of segments representing 1 to 13 years of exposure, increasing concentrations for only 3 out of 10 trace elements analysed, i.e. Cd, Pb and Zn. The constant concentrations of Fe, As, Co, Cu, Mn and Ni with the course of exposure time in their study does not comply with the increase in branch SIRM with time

of exposure, with SIRM being mainly dominated by the presence of iron rich particles. Although Drava et al. (2007) suggest that annual branch segments can be a good indicator for year-to-year atmospheric presence of Pb and Cd, we conclude from our data that trends in branch SIRM from current-year to three-year old branches of London plane cannot be used as indicator for year-to-year variation in magnetic particle concentrations, due to evolution of the branch surface structure with time. Maybe it is possible to evaluate the year-to-year particle accumulation on older branches which have completely shed the epidermis, but this certainly deserves further study.

4.4. Comparison of branch SIRM with leaf SIRM

With a median value of 106 x 10^{-6} A and a range of 18 - 650 x 10^{-6} A for Y_0 to Y_2 branches, the branch SIRM values obtained in our study are situated in the higher section of the range of SIRM values of leaves collected at similar urban sites from deciduous trees at the end of summer. For example, Hofman et al. (2013) found SIRM values of *P. x acerifolia* leaves, sampled between 5 and 12 m height, to range from 4 to 64 x 10^{-6} A in a street canyon in a medium-size Belgian city. In that same city, Kardel et al. (2012) measured, between 1.5 and 5 m height, mean leaf SIRM of 86, 99 and 46 x 10^{-6} A for *Carpinus betulus*, *Tilia* sp. with 'hairy' leaves and *Tilia* with 'non-hairy' leaves, respectively. In a study by Mitchell & Maher (2009) in Lancaster (UK), *Tilia platyphyllos* leaves from a suburban park and a heavily-trafficked section of a ring road, displayed at 1.5-2 m height mean SIRM values of 3 and 81 x 10^{-6} A, respectively. Of course, the branch SIRM in our study is elevated by the presence of 'older' branches in our dataset, which are exposed longer than one growing season and bared higher SIRM values. Indeed, our branch SIRM values are more in line with the leaf SIRM values of 34 to 640 x 10^{-6} A obtained by Hofman et al. (2014b) in Antwerp city from the evergreen climber *Hedera* sp., whose leaves are, like branches, exposed to air pollution throughout (multiple) entire year(s). Also, the median SIRM of the 'youngest' current-year branches (68 x 10^{-6} A) in our study is of the same order of magnitude as the above-mentioned leaf SIRM values of deciduous trees.

More correct is to compare SIRM values of branches and leaves normalized by exposed surface, as accumulation of particles occurs on both leaf sides (so considering the total leaf area instead of the one-sided leaf area). For example, Flanagan et al. (1980) found that twigs of roadside shrubs have higher traffic-derived lead and zinc accumulation per area than their leaves, when considering both abaxial and adaxial leaf surfaces. In a wind tunnel study by Freer-Smith et al. (2004), both deposition velocity and capture efficiency of particles were found larger for stems than leaves (at both sides) in deciduous trees with narrow stems, complex architecture and large simple leaves. It is not unlikely that next to object dimensions (Freer-Smith et al. 2004) differences in other surface

features (such as surface roughness and wettability) between branches and leaves could induce differences in particle accumulation between the surfaces. Although our magnetic values suggest that particle accumulation on current-year branches has the same order of magnitude as on leaves, a proper comparison of particle deposition and accumulation between co-located, simultaneously exposed branch and leaf surfaces is needed to evaluate their relative importance in PM removal at tree level.

4.5. Implications and suggestions

Based on our observations that branch bark, just like leaves, accumulates atmospheric particles and that their magnetic signal enables differentiating between sites differently exposed to traffic-related particles, we can conclude that deciduous tree branches provide a suitable exposure surface for biomonitoring purposes. The magnetic signal of branches can be used as proxy for time-integrated magnetic particle exposure, e.g. in pre-screening applications to identify hotspots and regions of interest for detailed analyses using more time-consuming and expensive methods. And although the use of branches instead of leaves has some advantages, it also has some drawbacks. Although branch SIRM is subject to more noise in comparison with leaves, branches have the advantage of being available in times when deciduous trees are leafless, e.g. due to drought or in wintertime conditions when air pollution often reaches even higher levels than in the growing season. The use of branches over leaves of evergreen broadleaf species like *Hedera* has the advantage that the surface's exposure time is known, although it is more difficult for species with Lammas growth. In practice, the effort for sampling and magnetic measurement of tree branches is similar as for leaves, but sample handling (cutting the branches into pieces that fit the sample holder) and manual determination of total surface areas for normalization is more time consuming and probably more prone to errors and contamination for branches than for leaves. The time-consuming surface area determination can be easily overcome by automatic measurements of projected surface areas, e.g. with scanners. Contamination during sample processing can be avoided easily by using metal-free secateurs and gloves. The most important weakness of the use of branches is the variation of the SIRM values with branch age. At least for London plane, our study shows that SIRM of branches of different ages cannot be used as indicator for temporal variation in PM concentrations, due to branch exfoliation. This however does not hamper the use of branch SIRM for biomonitoring studies to evaluate the spatial variation in particle exposure as long as the same branch age is sampled throughout the study. For next biomonitoring campaigns using branch magnetism, we suggest that sampling height, crown depth and particularly branch age are kept constant or, at least, are corrected for. Just as with leaves, biomonitoring with branches is limited by the availability of a

tree species in the city. This could be overcome by using multiple species based on inter-species calibration of branch SIRM, as established for leaves by Mitchell et al. (2010) and Kardel et al. (2011), or by combination with artificial samplers (Cao et al. 2015). Next to enabling magnetic screening, the epidermis or bark of branches has proven to be a suitable collection surface for particles which can be characterised by SEM and EDX. Our results provide the first indication that branches can be a valuable alternative for leaf magnetic biomonitoring, particularly in combination with SEM-EDX, but has some weaknesses related to inter-tree variation and sample handling effort. Further research is needed to confirm the capacity of wintertime branch SIRM to discriminate between multiple locations in a broad range of PM levels, and to determine the relationship of branch magnetic properties with total deposited particle mass and air concentrations of PM in particular. In addition, measurements of other branch magnetic parameters (such as magnetic susceptibility) will yield more information than SIRM alone on branch-accumulated particles, such as particle magnetic mineralogy and grain size, which could be useful for source-apportionment.

5. Conclusions

As hypothesized, magnetic particles are deposited on the epidermis and bark of branches of urban trees. Significant spatial intra- and inter-tree variation patterns were observed for branch SIRM, similar as seen for leaf SIRM in other studies, confirming our second hypothesis. The branch SIRM varied between trees in response to locations that differ in exposure to traffic-borne particles, rich in Fe and trace metals such as Cu, Cr and Zn. Significant variation in branch SIRM occurred within trees, due to location of the branch within the tree and its age. With increasing age, tree branches keep on accumulating magnetic particles for several years, for as branch SIRM tends to increase with each year of exposure, confirming our third hypothesis. However, changes in branch surface structure occur over time (i.e. epidermis shedding when branches are three years old), explains that trends in SIRM of branches developed in subsequent years cannot be used as indicators for year-to-year variation in atmospheric particle concentrations. On the practical side, the use of branches as biomagnetic indicator has some important drawbacks in comparison with the use of leaves: sample preparation requires more handling, and is thus more time-consuming and more prone to errors for branches than for leaves. Our results provide indications that, in atmospheric pollution screening programs, branches can be a valuable alternative for magnetic biomonitoring of particle pollution in seasons when deciduous trees are leafless. However, our study also highlights the practical considerations and limits of the methodology and the importance of inter-tree variation in branch SIRM (due to height, crown depth and branch age effects), which should be kept in mind when sampling in future air quality screening studies using branch (bark) biomagnetism.

Acknowledgements

We would like to thank the city council services of the city of Antwerp for their logistical support. We are grateful to Ana Castanheiro and Leen Van Ham for laboratory and SEM assistance. JH is supported as postdoctoral fellow of the Research Foundation Flanders (FWO; 12I4816N) and SVW is supported by a Marie Skłodowska-Curie Individual Fellowship.

References

Akima H., Gebhardt A., 2015. akima: Interpolation of irregularly and regularly spaced data. R package version 0.5-12. http://CRAN.R-project.org/package=akima

Cao L., Appel E., Hu S., Ma M., 2015. An economic passive sampling method to detect particulate pollutants using magnetic measurements. Environmental Pollution 205, 97–102.

Castanheiro A., Samson R., De Wael K., 2016. Magnetic- and particle-based techniques to investigate metal deposition on urban green. Science of The Total Environment 571, 594–602.

Catinon M., Ayrault S., Clocchiatti R., Boudouma O., Asta J., Tissut M., Ravanel P., 2009. The anthropogenic atmospheric elements fraction: A new interpretation of elemental deposits on tree barks. Atmospheric Environment 43, 1124–1130.

Drava G., Brignole D., Giordani P., Minganti V., 2017. The bark of the branches of holm oak (*Quercus ilex* L.) for a retrospective study of trace elements in the atmosphere. Environmental Research 154, 291–295.

Flanagan J.T., Wade K.J., Currie A., Curtis D.J., 1980. The deposition of lead and zinc from traffic pollution on two roadside shrubs. Environmental Pollution (Series B) 1, 71-78.

Flanders P.J., 1994. Collection, measurement, and analysis of airborne magnetic particulates from pollution in the environment. Journal of Applied Physics 75, 5931–5936.

Freer-Smith P.H., El-Khatib A.A., Taylor G., 2004. Capture of particulate pollution by trees: a comparison of species typical of semi-arid areas (*Ficus nitida* and *Eucalyptus globulus*) with European and North American species. Water, Air, and Soil Pollution 155,173–187.

Freer-Smith, P.H., Beckett, K.P., Taylor, G., 2005. Deposition velocities to *Sorbus aria, Acer campestre, Populus deltoides x trichocarpa 'Beaupré', Pinus nigra* and x *Cupressocyparis leylandii* for coarse, fine and ultra-fine particles in the urban environment. Environmental Pollution 133, 157-167.

Hansard R., Maher B.A., Kinnersley R., 2011. Biomagnetic monitoring of industry-derived particulate pollution. Environmental Pollution 159, 1673–1681.

Hoffmann V., Knab M., Appel E., 1999. Magnetic susceptibility mapping of roadside pollution. Journal of Geochemical Exploration 66, 313–326.

Hofman J., Bartholomeus H., Calders K., Van Wittenberghe S., Wuyts K., Samson R., 2014a. On the relation between tree crown morphology and particulate matter deposition on urban tree leaves: A ground-based LiDAR approach. Atmospheric Environment 99, 130-139.

Hofman J., Lefebvre W., Janssen S., Nackaerts R., Nuyts S., Mattheyses L., Samson R., 2014b. Increasing the spatial resolution of air quality assessments in urban areas: A comparison of biomagnetic monitoring and urban scale modelling. Atmospheric Environment 92, 130–140.

Hofman J., Stokkaer I., Snauwaert L., Samson R. (2013). Spatial distribution assessment of particulate matter in an urban street canyon using biomagnetic leaf monitoring of tree crown deposited particles. Environmental Pollution 183, 123-132.

691 Hofman J., Wuyts K., Van Wittenberghe S., Brackx M., Samson R., 2014c. On the link between biomagnetic
692 monitoring and leaf-deposited dust load of urban trees: Relationships and spatial variability of
693 different particle size fractions. Environmental Pollution 189, 63–72.
694 Hofman J., Wuyts K., Van Wittenberghe S., Samson R., 2014d. On the temporal variation of leaf magnetic
695 parameters: Seasonal accumulation of leaf-deposited and leaf-encapsulated particles of a roadside tree
696 crown. Science of the Total Environment 493, 766–772.
697 Kardel F., Wuyts K., Maher B.A., Hansard R., Samson R., 2011. Leaf saturation isothermal remanent
698 magnetization (SIRM) as a proxy for particulate matter monitoring: Inter-species differences and in-
699 season variation. Atmospheric Environment 45, 5164–5171.
700 Kardel F., Wuyts K., Maher B.A., Samson R., 2012. Intra-urban spatial variation of magnetic particles:
701 Monitoring via leaf saturation isothermal remanent magnetisation (SIRM). Atmospheric Environment
702 55, 111–120.
703 Kletetschka G., Ila V., Wasilewski P.J., 2003. Magnetic anomalies on the tree trunks. Studia Geophysica et
704 Geodaetica 47, 371−379.
705 Lehndorff E., Urbat L., Schwark L., 2006. Accumulation histories of magnetic particles on pine needles as
706 function of air quality. Atmospheric Environment 40, 7082–7096.
707 Matzka J., Maher B.A. (1999). Magnetic biomonitoring of roadside tree leaves: identification of spatial and
708 temporal variations in vehicle-derived particulates. Atmospheric Environment 33, 4565−4569.
709 McIntosh G., Gómez-Paccard M., Osete M.L., 2007. The magnetic properties of particles deposited on
710 *Platanus x hispanica* leaves in Madrid, Spain, and their temporal and spatial variations. Science of the
711 Total Environment 382, 135–146.
712 Mitchell R., Maher B.A., 2009. Evaluation and application of biomagnetic monitoring of traffic-derived
713 particulate pollution. Atmospheric Environment 43, 2095–2103.
714 Mitchell R., Maher B.A., Kinnersley R., 2010. Rates of particulate pollution deposition onto leaf surfaces:
715 Temporal and inter-species magnetic analyses. Environmental Pollution 158, 1472–1478.
716 Moreno E., Sagnotti L., Dinarès-Turell J., Winkler A., Cascella A., 2003. Biomonitoring of traffic air
717 pollution in Rome using magnetic properties of tree leaves. Atmospheric Environment 37, 2967–2977.
718 Muxworthy A.R., Matzka J., Davilab A.F., Petersen N., 2003. Magnetic signature of daily sampled urban
719 atmospheric particles. Atmospheric Environment 37, 4163–4169.
720 Pant P., Harrison R.M., 2013. Estimation of the contribution of road traffic emissions to particulate matter
721 concentrations from field measurements: A review. Atmospheric Environment 77, 78–79.
722 Pinheiro J., Bates D., DebRoy S., Sarkar D., R Core Team, 2015. nlme: Linear and Nonlinear Mixed Effects
723 Models. R package version 3.1-120, URL: http://CRAN.R-project.org/package=nlme.
724 R Core Team, 2015. R: A language and environment for statistical computing. R Foundation for Statistical
725 Computing, Vienna, Austria. URL http://www.R-project.org/
726 Rodríguez-Germade I., Mohamed K.J., Rey D., Rubio B., García A., 2014. The influence of weather and
727 climate on the reliability of magnetic properties of tree leaves as proxies for air pollution monitoring.
728 Science of the Total Environment 468–469, 892–902.

729 Sant'Ovaia H., Lacerda M.J., Gomes C., 2012. Particle pollution – An environmental magnetism study using
730 biocollectors located in northern Portugal. Atmospheric Environment 61, 340–349
731 Schädlich, G., Weissflog, L., Schüürmann, G., 1995. Magnetic susceptibility in conifer needles as indicator
732 of fly ash deposition. Fresenius Environmental Bulletin 4, 7–12.
733 SGS, 2010. Strategische Geluidsbelastingskaarten Agglomeratie Antwerpen, 090357-2-v1. SGS, Belgium
734 NV.
735 Szönyi M., Sagnotti L., Hirt A.M., 2008. A refined biomonitoring study of airborne particulate matter
736 pollution in Rome, with magnetic measurements on *Quercus ilex* tree leaves. Geophysical Journal
737 International 173, 127–141.
738 Urbat M., Lehndorff E., Schwark L., 2004. Biomonitoring of air quality in the Cologne conurbation using
739 pine needles as a passive sampler—Part I: magnetic properties. Atmospheric Environment 38, 3781–
740 3792.
741 Flanders Environment Agency 2013. Luchtkwaliteit in het Vlaamse Gewest – Jaarverslag
742 immissiemeetnetten – 2012 [in Dutch], 184 pp.
743 Flanders Environment Agency 2017. Luchtkwaliteit in de Antwerpse haven en de Antwerpse agglomeratie –
744 jaarrapport 2016 [in Dutch], 150 pp.
745 Vercauteren J., Matheeussen C., Wauters E., Roekens E., van Grieken R., Krata A., Makarovska Y.,
746 Maenhaut W., Chi X., Geypens B., 2011. Chemkar PM10: An extensive look at the local differences
747 in chemical composition of PM10 in Flanders, Belgium. Atmospheric Environment 45, 108–116.
748 Viana M., Kuhlbusch T.A.J., Querol X., Alastuey A., Harrison R.M., Hopke P.K., Winiwarter W., Vallius
749 M., Szidat S., Prévôt A.S.H., Hueglin C., Bloemen H., Wåhlin P., Vecchi R., Miranda A.I., Kasper-
750 Giebl A., Maenhaut W., Hitzenberger R., 2008. Source apportionment of particulate matter in Europe:
751 A review of methods and results. Aerosol Science 39, 827–849.
752 Vranckx S., Lefebvre W., 2013. Actualisering en verfijning luchtkwaliteitskaarten Stad Antwerpen [in
753 Dutch]. Final Report. Study commissioned by the City of Antwerp, 2013/RMA/R/318, VITO, 97 pp.
754 Wang L., Gong H., Liao W., Wang Z., 2015. Accumulation of particles on the surface of leaves during leaf
755 expansion. Science of the Total Environment 532, 420-434.
756 Wickham H. ggplot2: elegant graphics for data analysis. Springer New York, 2009.
757 Zhang C., Huang B., Piper J.D.A., Luo R., 2008. Biomonitoring of atmospheric particulate matter using
758 magnetic properties of *Salix matsudana* tree ring cores. Science of the Total Environment 393, 177–
759 190.